Hindawi Publishing Corporation
International Journal of Photoenergy
Volume 2008, Article ID 534038, 9 pages
doi:10.1155/2008/534038

Research Article

Preparation of Fluorine-Doped TiO_2 Photocatalysts with Controlled Crystalline Structure

N. Todorova,[1] T. Giannakopoulou,[1] G. Romanos,[2] T. Vaimakis,[3] Jiaguo Yu,[4] and C. Trapalis[1]

[1] *Institute of Materials Science, National Center for Scientific Research (NCSR) "Demokritos", 15310 Attica, Greece*
[2] *Institute of Physical Chemistry, National Center for Scientific Research (NCSR) "Demokritos", 15310 Attica, Greece*
[3] *Department of Chemistry, University of Ioannina, 45110 Ioannina, Greece*
[4] *State Key Laboratory of Advanced Technology for Materials Synthesis and Processing, Wuhan University of Technology, Wuhan 430070, China*

Correspondence should be addressed to C. Trapalis, trapalis@ims.demokritos.gr

Received 1 September 2007; Accepted 13 December 2007

Recommended by M. Sabry Abdel-Mottaleb

Nanocrystalline F-doped TiO_2 powders were prepared by sol-gel route. The thermal behavior of the powders was recorded by DTA/TG technique. The crystalline phase of the fluorinated TiO_2 powders was determined by X-ray diffraction technique. It was demonstrated that F-doping using CF_3COOH favors the formation of rutile along with anatase phase even at low temperature. Moreover, the rutile's phase content increases with the increase of the quantity of the fluorine precursor in the starting solution. The surface area of the powders and the pore size distribution were studied by N_2 adsorption-desorption using BET and BJH methods. X-ray photoelectron spectroscopy (XPS) revealed that the fluorine is presented in the TiO_2 powders mainly as metal fluoride in quantities ~16 at %. The F-doped TiO_2 showed a red-shift absorption in UV-vis region which was attributed to the increased content of rutile phase in the powders. The powders exhibited enhanced photocatalytic activity in decomposition of acetone.

1. INTRODUCTION

In the last decades, the TiO_2 is regarded as a promising material for organic pollutants remediation due to its properties [1]. Its wide application though is still retarded by the low efficiency of the photo-oxidative process. The development of titania-based photocatalysts activated by visible light ($\lambda \geq 385$ nm) remains a great challenge. Anion doping of TiO_2 films and powders with elements like nitrogen [2–5], sulfur [6, 7], carbon [8, 9], and fluorine [10–18] has been investigated in order to red-shift the absorbance to be achieved. Narrowing of the band gap of TiO_2 upon doping was often considered responsible for the enhanced visible light activity of these materials. Theoretical DOS calculations revealed intermediate energy levels available in the band gap of TiO_2 for most of the elements except fluorine [1]. Park and Choi [10] reported that surface fluorination (F-TiO_2) enhances the photocatalytic degradation of certain substrates due to the electron-trapping sites formation. The enhanced photocatalytic activity of F-doped powders has been attributed by Li et al. [11–13] to several beneficial effects produced by F-doping and mainly to the creation of surface oxygen vacancies. Yu et al. [14] reported fluorine ions incorporation in the TiO_2 lattice using an NH_4F source. They attributed the stronger absorption in the UV-visible range to the presence of the F^- ions that favor anatase phase formation and improve the crystallinity of TiO_2. However, Yamaki et al. [15] claimed that F-doping causes a modification of the conduction band edge and introduction of impurity states near its bottom. Our recent study on fluorine-modified titania films [18] revealed improved anatase crystallinity upon fluorine doping without the effective band gap of TiO_2 to be affected.

Anatase is usually produced when TiO_2 is synthesized by sol-gel method [19]. Calcination of anatase at high temperatures is applied to obtain rutile phase. Mixtures of anatase and rutile (e.g., Degussa P25 consists of ~75% anatase and ~25% rutile) are reported to exhibit enhanced photocatalytic activity in degradation of organic pollutants as the electron-hole recombination rate is decreased in the composite system [20]. Cheng et al. [21] reported that rutile phase is developed

preferably from a solution with low pH. Klein et al. [22] produced rutile (100%) titania powders at low temperature using nitric and hydrochloric acids as catalysts.

In this work, we study the influence of CF_3COOH fluorine precursor on the structure and the properties of TiO_2 powders.

2. EXPERIMENTAL

Fluorine- (F-) doped TiO_2 powders have been prepared by sol-gel route. Tetraethyl orthotitanate (TEOTi) Merck was used as titanium source. Different amounts of fluoroacetic acid (*Aldrich* Chemical Co., Milwaukee, Wis, USA) (atomic ratios F/Ti = 0, 10/90, 20/80) were dissolved in deionized water (molar ratio H_2O/TEOTi = 18) under stirring at room temperature and the TEOTi was added to the solution dropwise. The sols were stirred in closed beakers at room temperature for 24 hours for completion of the hydrolysis process. Consequently, they were dried at 90°C in air for 12 hours for water and alcohol evaporation. The xerogels obtained were denoted as TF0, TF10, and TF20 for the undoped TiO_2 and the samples with F/Ti = 10/90 and 20/80 atomic ratios, respectively. The as-prepared xerogels were calcinated at 400, 500, and 600°C for 1 hour in a Carbolite muffle furnace with heating rate of 5°C/min.

Differential thermal analysis (DTA) and thermogravimetry (TG) measurements were performed using NETZSCH equipment model STA 449. The samples with a mass ~14 mg were placed in alumina crucible and heated in air flow (30 mL/min) from room temperature up to 1000°C. The heating rate applied was 10°C/min.

The crystalline structure of the powders was investigated using X-ray diffraction (XRD) technique. SIEMENS D500 diffractometer with secondary graphite monochromator and CuKα radiation was used to obtain the X-ray diffraction patterns of the samples. The measurements were performed using the following combination of slits: 1.0°/1.0°/1.0° as aperture diaphragms, 0.15° as detector diaphragm, and 0.25° as diffracted beam monochromator diaphragm. The measured 2θ range between 20° and 80° was scanned in steps of 0.03°/2s. The size of the crystallites responsible for the Bragg reflection was determined using the Scherrer equation

$$d = \frac{k\lambda}{b\ \cos\theta}, \tag{1}$$

where d is the crystallite diameter in Å, k the shape constant (0.9), λ the wavelength in Å, θ the Bragg angle in degrees, and b the observed peak width at half-maximum peak height in rad. The phase content (%) of the samples was calculated using the formula [14]

$$W_R = \frac{A_R}{K_A A_A + A_R}, \tag{2}$$

where W_R is the content of the rutile phase ($W_A = 100 - W_R$), A_A and A_R are the integrated intensities of anatase (101) and rutile (110) peaks, respectively, and K_A is a coefficient equal to 0.886.

The surface areas of the powders were determined by the Branauer-Emmet-Teller (BET) method. The equipment COULTER 5200 USA was used for the nitrogen adsorption/desorption measurements at 77 K. All the samples were degassed at 573 K for 24 hours.

The presence of the fluorine in the TiO_2, the valence state of the dopant, as well as the bonding element was analyzed by X-ray photoelectron spectroscopy (XPS). Nonmonochromatized MgKα X-rays from a dual-anode VSW TA-10 source were used. The ultra-high vacuum (UHV) chamber was baked at 150°C for 12 hours to reach the 10^{-10} mbar pressure range. Measurements were performed for the samples without Ar ion sputtering (as received), as well as after a 45-minute light Ar^+ ion sputtering in order to remove most of the superficial carbon contamination.

UV-vis diffuse reflectance spectra of the samples in the wavelength range 200–900 nm were obtained using a UV-2100 Shimadzu instrument. The widths of the effective band gap of the samples were determined using Kubelka-Munk phenomenological theory [23].

The photocatalytic activity of the powders was evaluated by photocatalytic oxidation of acetone (CH_3COCH_3) using a 7L reactor (INNOVA). An amount of 0.3 g of each powder was used for the preparation of aqueous suspensions which were placed in petri dishes and dried at 100°C for 2 hours. The samples were placed into the reactor where acetone was injected. The initial humidity in the reactor was controlled by dryer containing $CaCl_2$. The acetone vapour was allowed to reach adsorption equilibrium with the photocatalyst prior measurements. Its initial concentration was about 400 ppm. A 15 W UV lamp (Cole Parmer Instr. Co., Chicago, Ill, USA) was used for illumination. The illumination time applied was 60 minutes. The amounts of acetone, carbon dioxide, and water vapour in the reactor were monitored. During the photocatalytic reaction, the acetone concentration decreased steadily. The photocatalytic activity of the powders was quantitatively evaluated by comparing the apparent reaction rate constants k_a of the decomposition reactions given that the degradation of acetone is known to be a reaction of pseudo first order [19].

3. RESULTS AND DISCUSSION

The TG, DTG, and DTA curves of undoped and F-doped TiO_2 powders are presented in Figure 1. For the undoped TiO_2 (Figure 1(a)), it can be observed that the total loss of weight (~25%) took place in three not well-defined steps. The first is the main loss of weight (~22.3%) that took place between ~30 and ~180°C and it was related to the evaporation of water and alcohol included in the xerogel. The second (~2.5%) and the third (~0.4%) weak losses took place between ~180–430°C and ~430–675°C, respectively, during which the remained water and organics (~2.9%) were gradually removed from the powders. The DTA curve reveals a weak exothermic phenomenon from 400°C to 672°C and it was connected to the process of crystallization of anatase. The endothermic effect after 670°C and the shoulder at 732°C were attributed to the process of anatase to rutile transformation. The DTA, TG, and DTG curves of the TF10 fluorinated xerogel are presented in Figure 1(b). It can be observed that the addition of fluorine containing substance

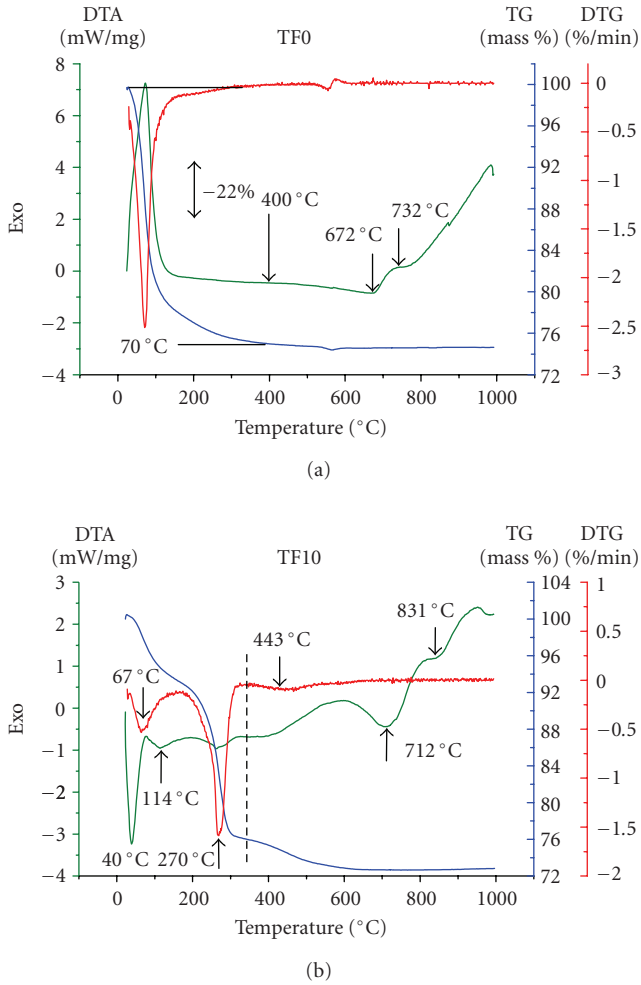

Figure 1: DTA, TG, DTG patterns of undoped (a) and fluorinated (b) titania powders.

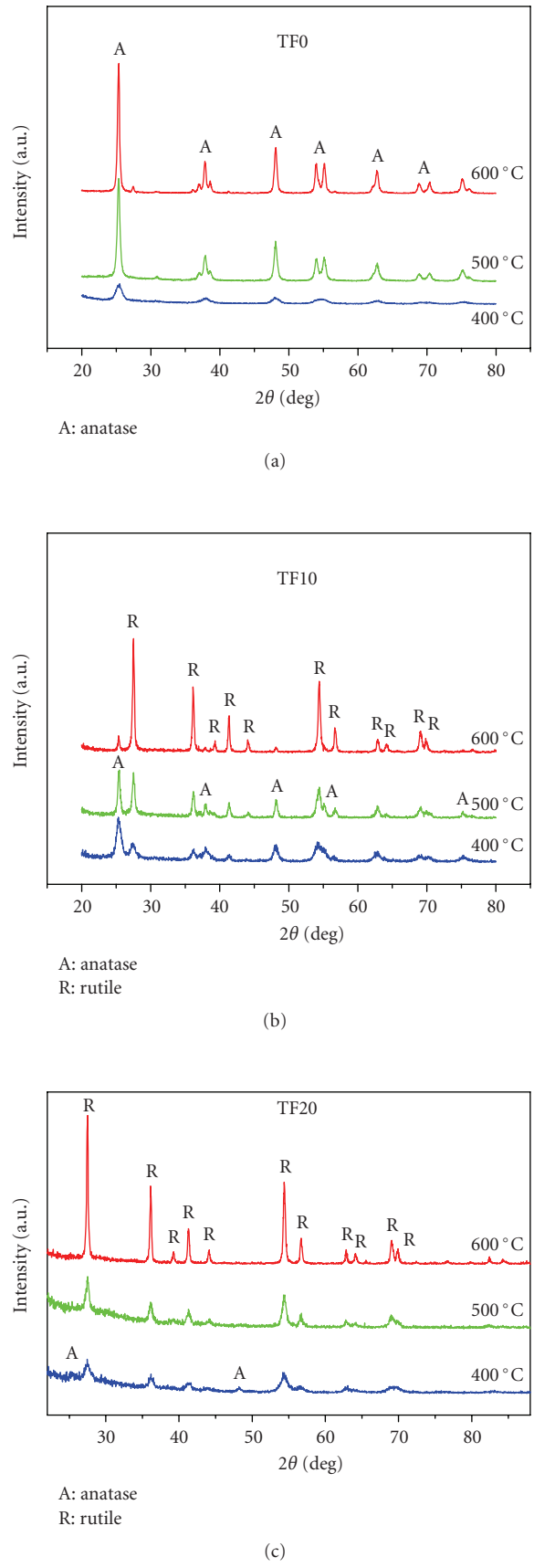

Figure 2: XRD patterns of undoped (a) and fluorinated TiO_2 powders with starting ratios F/Ti = 10/90 (b) and F/Ti = 20/80 (c).

results in complication of TG and DTA curves in comparison with the undoped sample. The mass decrease of the samples TCF10 took place in three steps. The first step of about 7.3% took place in the range of 30 to 150°C and the second step of about 17% took place from 150 to 350°C. The latter was connected to the decomposition and removal of organic radicals (CF_3COO^-). In addition, in the range from about 390 to 700°C, mass loss of about 3% took place that can be ascribed to the release of less volatile components and reaction products. Beyond ~700°C the DTA curve exhibits endothermic tendency which might be attributed to the anatase to rutile transformation. The thermal behavior of TF20 xerogel (not given) was similar to the TF10 sample.

The X-ray diffraction patterns of the calcinated at 400, 500, and 600°C samples are presented in Figure 2. In our study, pure anatase was recorded for the undoped titania (Figure 2(a)) after thermal treatment at every temperature mentioned above. The XRD patterns of F-doped TiO_2 powders (Figures 2(b) and 2(c)) revealed that a second crystalline phase, that of rutile, was developed along with the anatase phase at temperatures as low as 400°C. The average sizes of

Table 1: Phase content W (%) and average diameter d (nm) of the crystallites in the TiO_2 powders calcinated at different temperatures (A: Anatase, R: Rutile).

Nominal name	Calcination temperatures					
	400°C		500°C		600°C	
	W (%)	d (nm)	W (%)	d (nm)	W (%)	d (nm)
TF0 F/Ti = 0	A:100	8.5	A:100	12.0	A:100	18.0
TF10 F/Ti = 10/90	A:72.5 R:27.4	10.5 10.6	A:45.7 R:54.3	21.5 20.8	A:9.3 R:90.7	15.5 20.8
TF20 F/Ti = 20/80	A:9.1 R:90.9	10.2	R:100	14.1	R:100	36.1

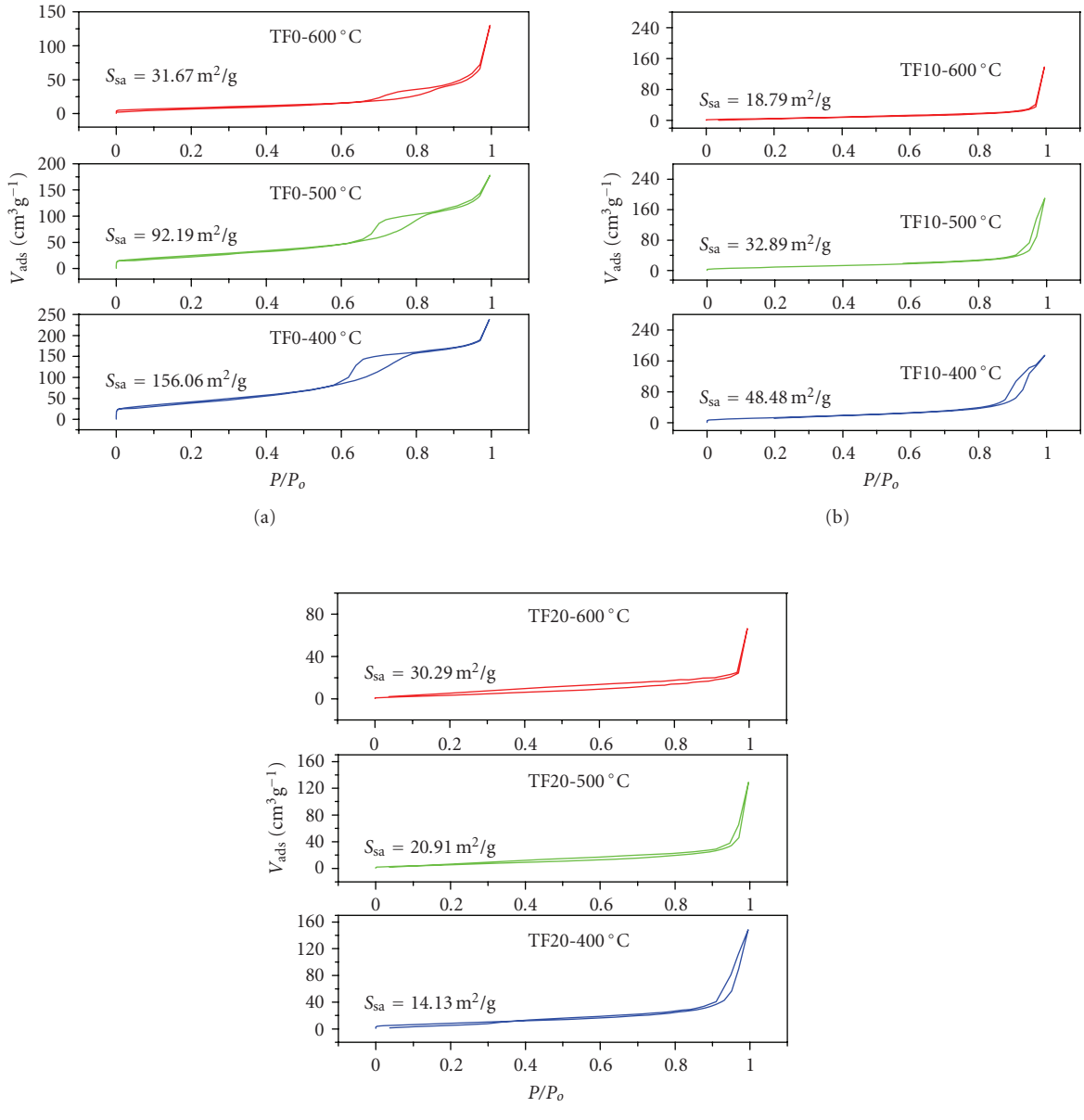

Figure 3: Nitrogen adsorption-desorption isotherms of undoped (a) and F-doped (b) and (c) powders calcinated at different temperatures.

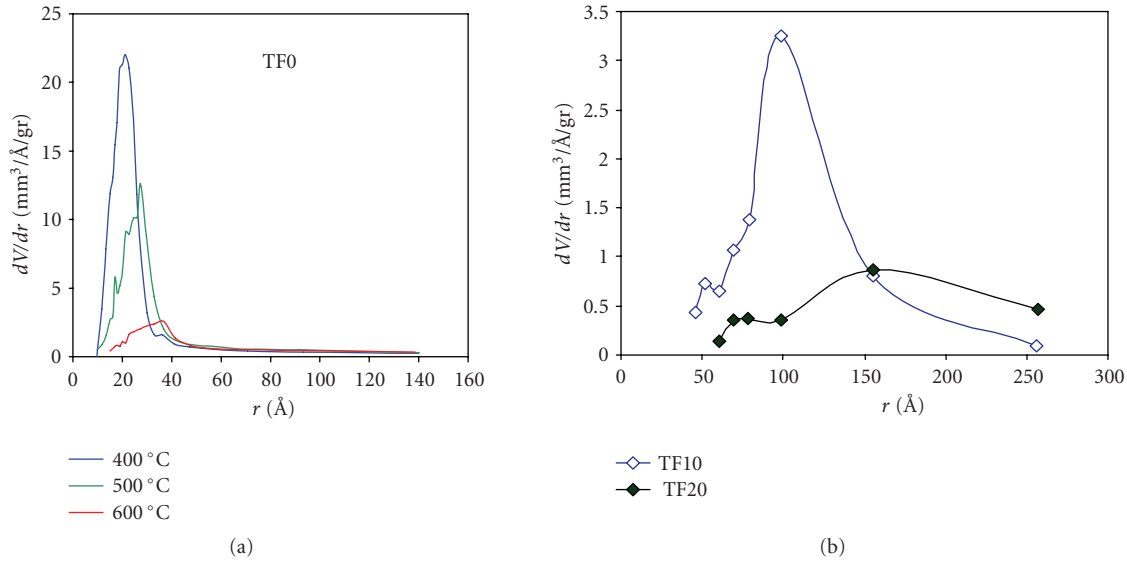

Figure 4: Pore size distribution in the undoped TiO_2 calcinated at different temperatures (a) and in the TF10 and TF20 powders calcinated at 400°C (b).

Table 2: BET surface area and porosity of TiO_2 powders calcinated at different temperatures.

Nominal name	Calcination temperatures					
	400°C		500°C		600°C	
	BET_{SSA} (m^2/g)	Porosity (%)	BET_{SSA} (m^2/g)	Porosity (%)	BET_{SSA} (m^2/g)	Porosity (%)
TF0 F/Ti = 0	156.06	55.34	92.19	47.77	31.67	32.34
TF10 F/Ti = 10/90	48.48	32.15	32.89	22.41	18.79	10.23
TF20 F/Ti = 20/80	14.13	22.57	20.91	13.06	30.29	7.32

the crystallites (d, nm), as well as the anatase/rutile phase composition (W, %) of the powders are presented in Table 1. From the results displayed in Figure 2 and Table 1, it is evident that the crystallization process of TiO_2 depends on the presence and the quantity of the fluorine precursor, as well as the calcination temperature. The increase in the size of the crystallites with the increase of the calcination temperatures can be observed for all the samples. It is also evident that the polymorph phase composition is dependent on the quantity of the CF_3COOH in the starting solution. It can be deduced that fluorine-doped titania powders with controlled anatase/rutile phase composition can be synthesized by altering the molar ratio of CF_3COOH/TEOTi in the starting solution and the calcination temperature.

The influence of the F^- ions on the crystallization process of TiO_2 has been studied and improved anatase crystallinity upon F-doping has been reported [14, 18]. Up to our knowledge, there is no report on direct synthesis and fluorination of TiO_2 powder with controlled anatase/rutile content. Moreover, the increase of the F/Ti molar ratio in the starting solution (sample TF20) leads to formation of pure rutile even at 400°C. The crystallization of rutile alone or along with anatase phase at low temperatures is attributed to the acidic character of the fluorine precursor which provides low pH conditions during peptization. At these acidic conditions, the edge-shared bonding among the $[TiO_6]$ octahedrons which is responsible for anatase formation during calcination is suppressed, while the corner-shared bonding that is responsible for the rutile formation is favored [21].

Nitrogen adsorption-desorption isotherm measurements were performed to determine the specific surface area, the porosity, and the pore size distribution in the samples. The N_2 adsorption-desorption isotherms for the undoped TiO_2 and the fluorinated samples calcinated at 400°C clearly show a *hysteresis* in the desorption branch (Figure 3). These samples exhibited the highest BET surface area. Their pore size distribution curves obtained from the desorption branch are depicted in Figure 4. From the figures and the results presented in Table 2, it can be observed that the BET surface areas decrease significantly while the pore size distribution becomes wider with the increase of the calcination temperature for all samples. A decrease in the

porosity with the increase of the calcination temperature is also evident. The BET values for the fluorinated powders are much lower than those for the undoped TiO_2 powders when calcinated at the same temperatures. These findings are connected to the presence of fluorine containing organic precursor in the xerogels and the exothermic phenomena of its burning occurring during calcination. The heat release leads to the agglomeration of TiO_2 nanoparticles and to the decrease of the BET surface area. The process contributes to the improvement of the TiO_2 crystallinity as it was revealed by XRD results.

The chemical composition of the sample TF20 calcinated at 400°C was studied by XPS analysis. After the removal of the superficial carbon contaminant (3-4 monolayers), the elements detected were titanium, oxygen, and fluorine. The spectra obtained for Ti 2p, O 1s, and F 1s regions (Figure 5) revealed that the powder consists of TiO_2, where titanium and oxygen are present as Ti^{4+} and O^{2-}. The valence states of the titanium and the oxygen were determined from the Ti 2p3/2–Ti 2p1/2 splitting (~5.7 eV) and the difference of ~71.5 eV between the binding energies of the Ti 2p3/2 peak (458.5 ± 0.1 eV) and the O 1s peak (530.0 ± 0.1 eV). The F 1s spectrum (Figure 5(c)) is nonsymmetric and the contribution near 684.3 eV indicates that the fluorine is presented in the sample mainly as TiF_4 [24] and/or to physically adsorbed F^- on TiO_2 [19]. The contribution near 685.4 eV could be related to $TiOF_2$ structures [12] and the tail near 688 eV to nonstoichiometric solid solution of F in TiO_2 of the $TiO_{2-x}F_x$ type [12, 19]. It can be also associated with C–F bonding in CF_3 residual groups [25]. The fluorine concentration was estimated as ~14 at % before and ~16 at % after the Ar^+ ions sputtering. This level of doping can be connected to the high temperature of decomposition of the fluorine precursor which is evident from the thermal analysis.

The diffuse reflectance spectra (R) of the samples were used to assess the absorption of the photocatalysts in the UV-vis region. The undoped TF0 sample and the TF20 samples revealed typical anatase and rutile spectra, respectively, and for this reason they are not shown. The absorption curves of the fluorinated TF10 samples with various anatase/rutile ratios are presented in Figure 6(a). The P25 absorption curve is also presented for comparison because of its mixed phase composition (anatase ~75% and rutile ~25%). To determine the band gap of the powders, the Kubelka-Munk method based on the diffuse reflectance spectra was employed. The $(F(R)hv)^{1/2}$ versus hv plots of the P25 and the TF10 samples are presented in Figure 6(b), where $F(R) = (1-R)/2R$. It can be observed that the band gap values obtained for the Degussa P-25 and the TF10 sample calcinated at 400°C are close (3.08 eV and 3.07 eV, resp.). This fact can be connected to the similar anatase/rutile phase content of the samples. This is also consistent with the literature [11, 12, 19] and support the conception that the fluorine doping does not affect the band gap of TiO_2. With the increase of the calcination temperature, the widths of the band gap for the fluorinated samples decrease from 3.07 to 3.03 eV. This "narrowing" of the effective band gap is attributed to the increase of the rutile content in the powders which is in accordance with our XRD results.

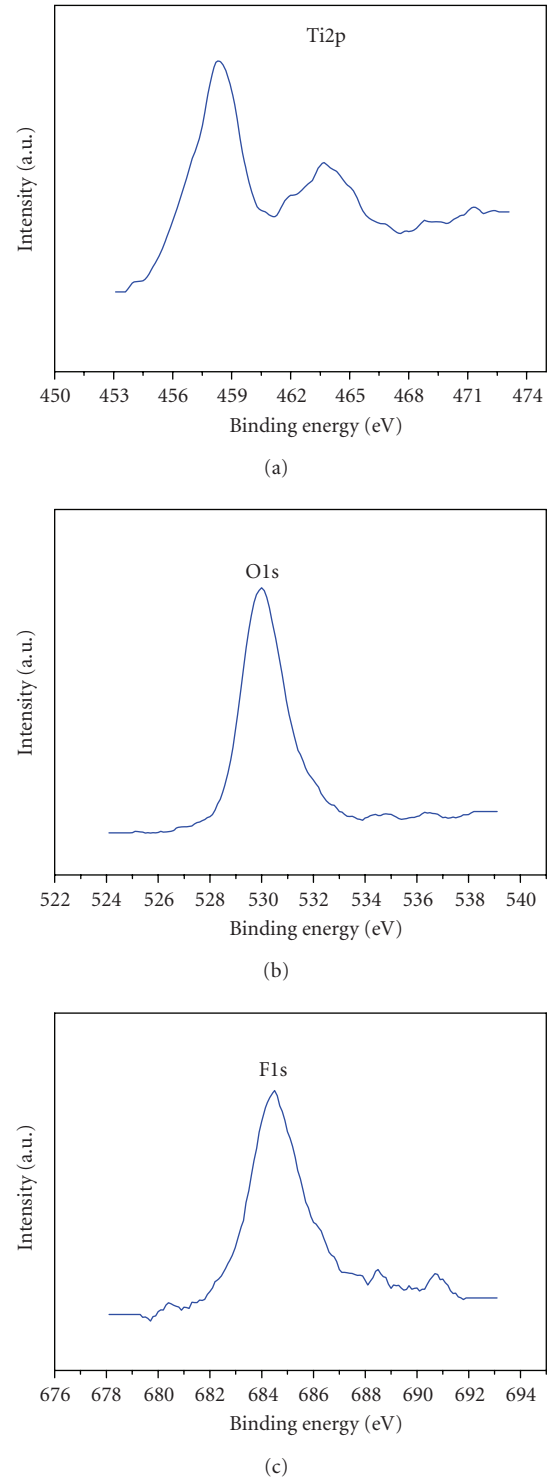

Figure 5: XPS spectra for Ti 2p (a), O 1s (b), and F 1s (c) regions of TF20 sample calcinated at 400°C.

The increase in the CO_2 concentration due to the decomposition of acetone and the calculated apparent rate constant of the photocatalytic reaction are presented in Figures 7 and 8, respectively. From our results, it can be concluded that the fluorinated TiO_2 powders exhibit enhanced activity in comparison to the reference photocatalyst Degussa P25.

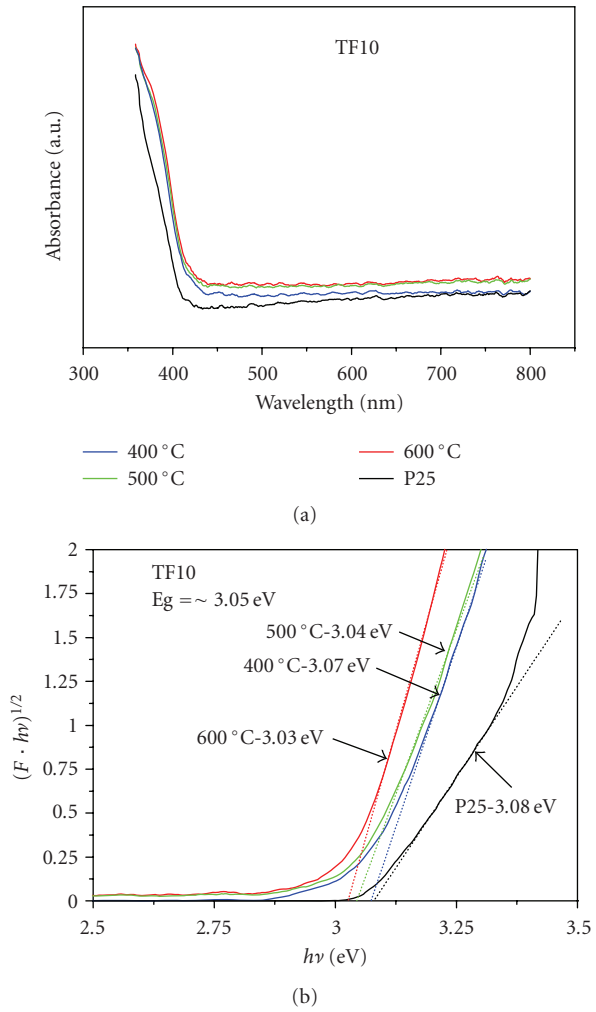

FIGURE 6: Absorbance spectra (a) and Kubelka-Munk plot for band gap evaluation (b) of fluorinated (TF10) TiO_2 and P25 powders.

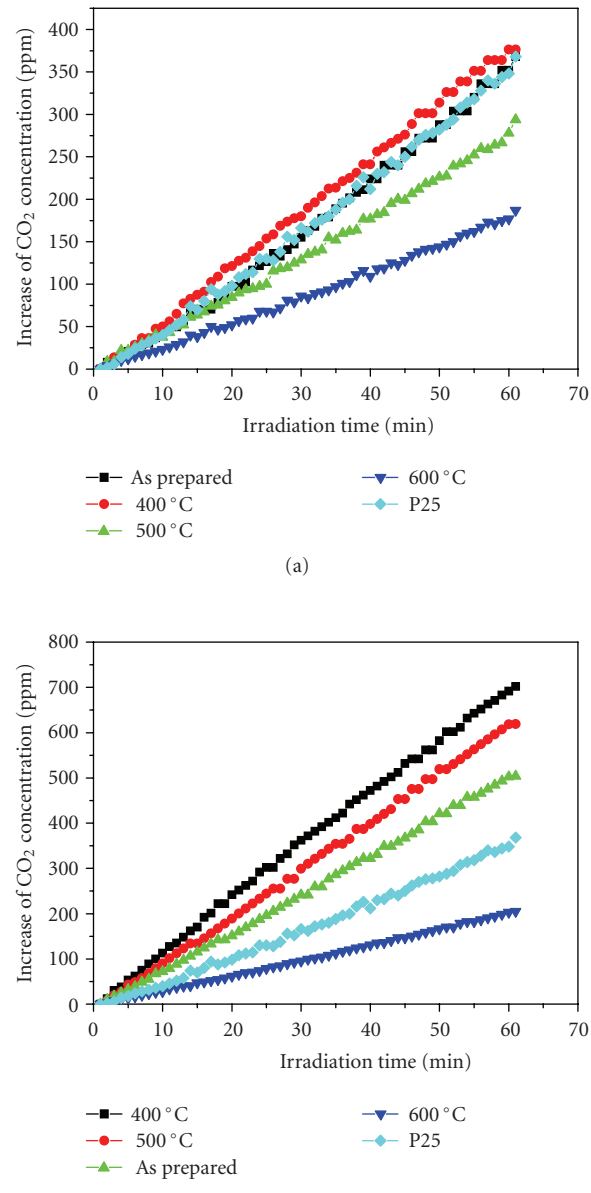

FIGURE 7: Increase of the CO_2 concentration due to decomposition of acetone for fluorinated TF10 (a) and TF20 (b) titania powders.

The best results are recorded for the powders calcinated at 400°C which can be connected to the mixed anatase/rutile phase composition and the higher BET surface area in comparison to the samples calcinated at 500 and 600°C. In addition, the activity of TF20 samples treated at 400 and 500°C exceeds significantly the activity of the corresponding TF10 powders. This fact was attributed to the rutile rich composition of the powders and the higher level of fluorine doping. The drastic decrease in the activity of the treated at 600°C samples is attributed to the decrease of the BET surface area, as well as to the absence of anatase phase in the powders.

4. CONCLUSIONS

Simultaneous fluorination and controlled low-temperature anatase/rutile phase crystallization of nanosized TiO_2 powders were achieved using sol-gel route. It was found that the anatase/rutile crystalline ratio depends on the amount of fluorine precursor used for fluorination as well as on the temperature of thermal treatment.

The crystallization of pure rutile or anatase/rutile mixture at low temperatures is attributed to the acidic character of the fluorine precursor. Improved crystallinity and enhanced absorbance of the powders in the UV-vis region are recorded upon F-doping. The fluorine is presented in the powders mainly as metal (Ti) fluoride.

The width of the TiO_2 band gap was not affected by the presence of fluorine. The red shift of the absorption edge is attributed to the increased rutile content in the fluorine doped TiO_2 powders. The prepared fluorine doped TiO_2 powders calcinated at 400°C exhibited higher photocatalytic activity than that of Degussa P-25 for decomposition of acetone under UV-vis illumination.

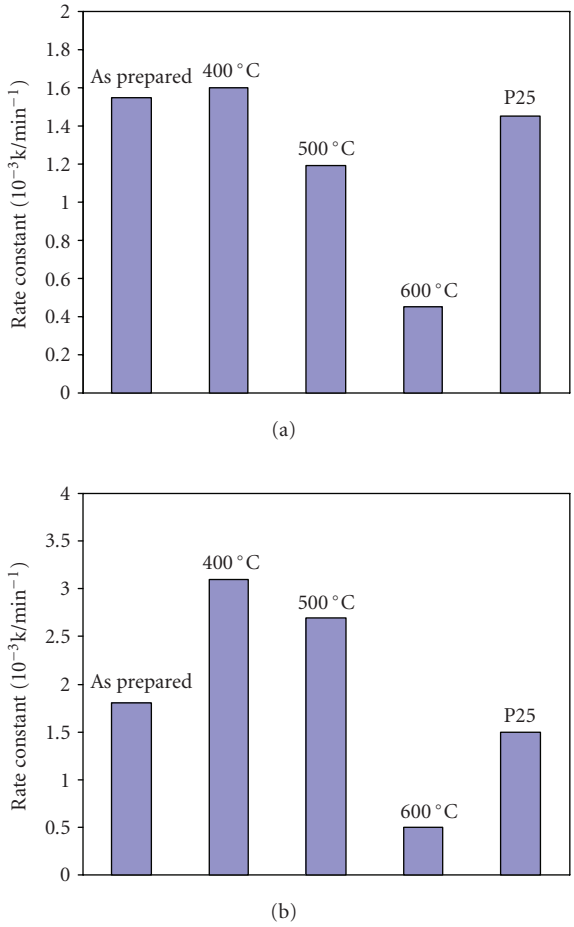

Figure 8: Photocatalytic activity of fluorinated TF10 (a) and TF20 (b) titania powders evaluated by decomposition of acetone.

ACKNOWLEDGMENTS

Financial support of National Secretariat for Research and Technology and the Ministry of Development, under Grant Non-EU 05 245 is gratefully acknowledged.

REFERENCES

[1] R. Asahi, T. Morikawa, T. Ohwaki, K. Aoki, and Y. Taga, "Visible-light photocatalysis in nitrogen-doped titanium oxides," *Science*, vol. 293, no. 5528, pp. 269–271, 2001.

[2] S. Sato, "Photocatalytic activity of NO_x-doped TiO_2 in the visible light region," *Chemical Physics Letters*, vol. 123, no. 1-2, pp. 126–128, 1986.

[3] J. L. Gole, J. D. Stout, C. Burda, Y. Lou, and X. Chen, "Highly efficient formation of visible light tunable $TiO_{2-x}N_x$ photocatalysts and their transformation at the nanoscale," *Journal of Physical Chemistry B*, vol. 108, no. 4, pp. 1230–1240, 2004.

[4] M. Batzill, E. H. Morales, and U. Diebold, "Influence of nitrogen doping on the defect formation and surface properties of TiO_2 rutile and anatase," *Physical Review Letters*, vol. 96, no. 2, Article ID 026103, 4 pages, 2006.

[5] V. Balek, D. Li, J. Šubrt, et al., "Characterization of nitrogen and fluorine co-doped titania photocatalyst: effect of temperature on microstructure and surface activity properties," *Journal of Physics and Chemistry of Solids*, vol. 68, no. 5-6, pp. 770–774, 2007.

[6] T. Ohno, M. Akiyoshi, T. Umebayashi, K. Asai, T. Mitsui, and M. Matsumura, "Preparation of S-doped TiO_2 photocatalysts and their photocatalytic activities under visible light," *Applied Catalysis A*, vol. 265, no. 1, pp. 115–121, 2004.

[7] T. Umebayashi, T. Yamaki, H. Itoh, and K. Asai, "Band gap narrowing of titanium dioxide by sulphur doping," *Applied Physics Letters*, vol. 81, no. 3, p. 454, 2002.

[8] T. Tachikawa, S. Tojo, K. Kawai, et al., "Photocatalytic oxidation reactivity of holes in the sulphur-and carbon-doped TiO_2 powders studied by time-resolved diffuse reflectance spectroscopy," *Journal of Physical Chemistry B*, vol. 108, no. 50, pp. 19299–19306, 2004.

[9] A. Hattori, K. Shimoda, H. Tada, and S. Ito, "Photoreactivity of sol-gel TiO_2 films formed on soda-lime glass substrates: effect of SiO_2 underlayer containing fluorine," *Langmuir*, vol. 15, no. 16, pp. 5422–5425, 1999.

[10] H. Park and W. Choi, "Effects of TiO_2 surface fluorination on photocatalytic reactions and photoelectrochemical behaviors," *Journal of Physical Chemistry B*, vol. 108, no. 13, pp. 4086–4093, 2004.

[11] D. Li, H. Haneda, S. Hishita, N. Ohashi, and N. K. Labhsetwar, "Fluorine-doped TiO_2 powders prepared by spray pyrolysis and their improved photocatalytic activity for decomposition of gas-phase acetaldehyde," *Journal of Fluorine Chemistry*, vol. 126, no. 1, pp. 69–77, 2005.

[12] D. Li, H. Haneda, N. K. Labhsetwar, S. Hishita, and N. Ohashi, "Visible-light-driven photocatalysis on fluorine-doped TiO_2 powders by the creation of surface oxygen vacancies," *Chemical Physics Letters*, vol. 401, no. 4–6, pp. 579–584, 2005.

[13] D. Li, N. Ohashi, S. Hishita, T. Kolodiazhnyi, and H. Haneda, "Origin of visible-light-driven photocatalysis: a comparative study on N/F-doped and N-F-codoped TiO_2 powders by means of experimental characterizations and theoretical calculations," *Journal of Solid State Chemistry*, vol. 178, no. 11, pp. 3293–3302, 2005.

[14] J. Yu, J. C. Yu, M. K.-P. Leung, et al., "Effects of acidic and basic hydrolysis catalysts on the photocatalytic activity and microstructures of bimodal mesoporous titania," *Journal of Catalysis*, vol. 217, no. 1, pp. 69–78, 2003.

[15] T. Yamaki, T. Umebayashi, T. Sumita, et al., "Fluorine-doping in titanium dioxide by ion implantation technique," *Nuclear Instruments and Methods in Physics Research B*, vol. 206, pp. 254–258, 2003.

[16] D. Huang, S. Liao, S. Quan, et al., "Preparation of anatase F doped TiO_2 sol and its performance for photodegradation of formaldehyde," *Journal of Materials Science*, vol. 42, no. 19, pp. 8193–8202, 2007.

[17] D. Huang, S. Liao, J.-M. Liu, Z. Dang, and L. Petrik, "Preparation of visible-light responsive N-F-codoped TiO_2 photocatalyst by a sol-gel-solvothermal method," *Journal of Photochemistry and Photobiology A*, vol. 184, no. 3, pp. 282–288, 2006.

[18] T. Giannakopoulou, N. Todorova, C. Trapalis, and T. Vaimakis, "Effect of fluorine doping and SiO_2 under-layer on the optical properties of TiO_2 thin films," *Materials Letters*, vol. 61, no. 23-24, pp. 4474–4477, 2007.

[19] J. C. Yu, J. Yu, W. Ho, Z. Jiang, and L. Zhang, "Effects of F^- doping on the photocatalytic activity and microstructures of nanocrystalline TiO_2 powders," *Chemistry of Materials*, vol. 14, no. 9, pp. 3808–3816, 2002.

[20] B. Sun and P. G. Smirniotis, "Interaction of anatase and rutile TiO_2 particles in aqueous photooxidation," *Catalysis Today*, vol. 88, no. 1-2, pp. 49–59, 2003.

[21] H. Cheng, J. Ma, Z. Zhao, and L. Qi, "Hydrothrmal preparation of uniform nanosize rutile and anatase particles," *Chemistry of Materials*, vol. 7, no. 4, pp. 663–671, 1995.

[22] S. M. Klein, J. H. Choi, D. J. Pine, and F. F. Lange, "Synthesis of rutile titania powders: agglomeration, dissolution, and reprecipitation phenomena," *Journal of Materials Research*, vol. 18, no. 6, pp. 1457–1464, 2003.

[23] E. L. Simmons, "Relation of the diffuse reflectance remission function to the fundamental optical parameters," *Journal of Modern Optics*, vol. 19, no. 10, pp. 845–851, 1972.

[24] T. Yamaki, T. Sumita, and S. Yamamoto, "Formation of $TiO_{2-x}F_x$ compounds in fluorine-implanted TiO_2," *Journal of Materials Science Letters*, vol. 21, no. 1, pp. 33–35, 2002.

[25] J. C. Yu, W. Ho, J. Yu, S. K. Hark, and K. Iu, "Effects of trifluoroacetic acid modification on the surface microstructures and photocatalytic activity of mesoporous TiO_2 thin films," *Langmuir*, vol. 19, no. 9, pp. 3889–3896, 2003.